Possible Metastable State Triggered by Competition of Peierls State and Charge Ordered State

Yukiko OMORI, Masahisa TSUCHIIZU, and Yoshikazu SUZUMURA

Department of Physics, Nagoya University, Nagoya 464-8602

(Received January 12, 2008; published in J. Phys. Soc. Jpn. **76** (2007) 114709)

We examine a Peierls ground state and its competing metastable state in the one-dimensional quarter-filled Peierls-Hubbard model with the nearest-neighbor repulsive interaction V and the electron-phonon interaction ($\propto 1/K$ with K being the elastic constant). From the mean-field approach, we obtain the phase diagram for the ground state on the plane of parameters V and K. The coexistent state of the spin-density wave and the charge ordering is realized for large V and K. With decreasing K, it exhibits a first-order phase transition to the unconventional Peierls state which is described by the bond-centered charge-density-wave state. In the large region of the Peierls ground state in the phase diagram, there exists the metastable state where the energy takes a local minimum with respect to the lattice distortion. On the basis of the present calculation, we discuss the photoinduced phase observed in the (EDO-TTF)$_2$PF$_6$ compound.

KEYWORDS: Peierls-Hubbard model, first-order phase transition, charge ordering, spin-density wave, quarter filling, metastable state, (EDO-TTF)$_2$PF$_6$

1. Introduction

Electron correlation in quasi-one-dimensional molecular conductors has been studied extensively[1,2] where the spin density wave (SDW) state with the momentum $2k_{\rm F}$ ($k_{\rm F}$ denotes the Fermi momentum) originates from the combined effect of repulsive interaction and the nesting of the Fermi surface. The former effect is relatively large in molecular conductors and the latter effect becomes perfect for the one-dimensional band. In particular, the quarter-filled band systems, which have been the main subject in molecular conductors, supply a rich variety of electronic states,[3] e.g., the charge ordering (CO)[4,5] with a periodic array of charge disproportionation (+1, 0, +1, 0, $\cdots$). In addition to the pure $2k_{\rm F}$ SDW, the coexistent state of the $2k_{\rm F}$ SDW and $2k_{\rm F}$ charge-density wave (CDW) has been observed in the X-ray experiment on (TMTSF)$_2$PF$_6$,[6,7] where the coexistent state has a purely electronic origin due to the absence of lattice distortion. It has been clarified theoretically that the next-nearest repulsive interaction gives rise to such a coexistence,[8,9] and that the state undergoes a first-order phase transition into the normal state with increasing temperature T.[10]

The molecular compound (EDO-TTF)$_2$PF$_6$, which is another salt showing a typical quasi-one-dimensional system, is a recent topic of the photoinduced phase transition.[11–14] It has been reported that the first-order phase transition from metal to the Peierls insulator occurs at $T \simeq 278$ K and is followed by the fourfold periodicity of the charge-rich sites and the charge-poor sites with the spatial variation of (+1, 0, 0, +1, $\cdots$). The large hysteresis is accompanied by the lattice distortion indicating the strong coupling to the lattice through the electron-phonon (e-p) interaction. This Peierls state shows a distinctive feature of the $2k_{\rm F}$ CDW where the amplitude of the lattice distortion takes a maximum between the hole-rich sites of the EDO-TTF molecules (i.e., the bond ordering). Although the spatial variation of the charge density is similar to the conventional CDW,[6–10] the spatial pattern of the lattice distortion found in (EDO-TTF)$_2$PF$_6$ has not been fully understood in the context of the previous theory.[15] Furthermore, the conductivity of (EDO-TTF)$_2$PF$_6$ exhibits a gigantic photoresponse, and the ultrafast insulator-to-metal transition is induced by the weak laser photoexcitation. The mechanism of this behavior has been discussed by assuming the existence of a metastable state without lattice distortion. However, it remains unclear if such a metastable state can be understood using the Peierls model in the presence of the electronic correlation.

In the present paper, we examine the possible origin of the metastable state, which arises from the interplay of the Peierls state and the CO state. In §2, the model with both the repulsive interactions and the e-p interaction is described and the formulation is given within the mean-field theory. In §3 and §4, the ground state and the metastable state are calculated to obtain the phase diagram. The possible parameter region for the metastable state is estimated. Section 5 is devoted to summary and discussions.

2. Formulation

We consider the 1/4-filled Peierls-Hubbard Hamiltonian given by[16,17]

$$\begin{aligned} H = & -t\sum_{j=1}^{N}\sum_{\sigma=\uparrow,\downarrow}(c_{j,\sigma}^{\dagger}c_{j+1,\sigma}+\text{H.c.}) \\ & +U\sum_{j}n_{j,\uparrow}n_{j,\downarrow}+V\sum_{j}n_{j}n_{j+1} \\ & +t\sum_{j\sigma}u_{j}(c_{j,\sigma}^{\dagger}c_{j+1,\sigma}+\text{H.c.}) \\ & +\frac{K}{2}\sum_{j}u_{j}^{2}+\frac{\delta K}{2}\sum_{\text{odd}\,j}u_{j}^{2}, \end{aligned} \tag{1}$$

where $c_{j,\sigma}$ (spin $\sigma=\uparrow,\downarrow$) is the annihilation operator of the electron at the site j and $n_j=\sum_\sigma c_{j,\sigma}^{\dagger}c_{j,\sigma}$. We impose the periodic boundary condition, $c_{j+N,\sigma}=c_{j,\sigma}$. Quantities U and V denote the on-site and nearest-neighbor-site repulsive interactions, respectively. The term proportional to u_j (corresponding to the lattice distortion) denotes the e-p interaction and

the last two terms represent the elastic energy with the elastic constant K and $K+\delta K$ for even and odd j, respectively. The alternating elastic constant given by δK plays a crucial role in the present paper. As for the lattice distortion u_j, we take into account only the modulation with the momentum $2k_{\rm F}(=\pi/2)$ (corresponding to the lattice tetramerization), which is relevant to the Peierls state in the (EDO-TTF)$_2$PF$_6$, and u_j is rewritten as

$$u_j = u_{\rm t}\cos\left(\frac{\pi}{2}j+\xi\right), \tag{2}$$

where $u_{\rm t}$ is the amplitude of the lattice tetramerization. The elastic constant K is scaled so as to include the e-p coupling constant. In the present paper, we do not consider the possibility of the lattice dimerization with the momentum $4k_F(=\pi)$.[15,18] Its detail is discussed in §5.

After applying the Fourier transform, we define order parameters ($m=0,1,2,3$) as[10]

$$S_{mQ_0} = \frac{1}{N}\sum_{\sigma=\uparrow,\downarrow}\sum_{-\pi<k\le\pi}{\rm sgn}(\sigma)\left\langle c^\dagger_{k,\sigma}c_{k+mQ_0,\sigma}\right\rangle_{\rm MF}, \tag{3}$$

$$D_{mQ_0} = \frac{1}{N}\sum_{\sigma=\uparrow,\downarrow}\sum_{-\pi<k\le\pi}\left\langle c^\dagger_{k,\sigma}c_{k+mQ_0,\sigma}\right\rangle_{\rm MF}, \tag{4}$$

where $Q_0=2k_{\rm F}=\pi/2$, $S_0=0$, $D_0=1/2$, and

$$S_{Q_0}=S^*_{3Q_0}\equiv S_1{\rm e}^{{\rm i}\theta},\quad D_{Q_0}=D^*_{3Q_0}\equiv D_1{\rm e}^{{\rm i}\theta'},$$
$$S_{2Q_0}=S^*_{2Q_0}\equiv S_2,\quad D_{2Q_0}=D^*_{2Q_0}\equiv D_2.$$

We note that S_1, S_2, D_1, and D_2 (which are real numbers) correspond to the amplitudes for the $2k_{\rm F}$ SDW, $4k_{\rm F}$ SDW, $2k_{\rm F}$ CDW, and $4k_{\rm F}$ CDW, respectively, and θ and θ' are the phases for the $2k_{\rm F}$ SDW and $2k_{\rm F}$ CDW. It has been found that the relation $\theta'=\pi/2+\theta$ holds for $u_{\rm t}=0$.[9] In terms of these order parameters, the mean-field Hamiltonian is written as

$$H_{\rm MF}=\sum_{k,\sigma}\left\{\left(\varepsilon_k+\frac{U}{4}+V\right)c^\dagger_{k,\sigma}c_{k,\sigma}+\left[\left(\Delta_{Q_0,\sigma}+\frac{1}{2}u_{\rm t}{\rm e}^{{\rm i}\xi}(1-{\rm i})(\cos k-\sin k)\right)c^\dagger_{k+Q_0,\sigma}c_{k,\sigma}+{\rm H.c.}\right]+\Delta_{2Q_0,\sigma}c^\dagger_{k,\sigma}c_{k+2Q_0,\sigma}\right\}$$
$$-\frac{N}{4}\left[U\left(\frac{1}{4}+2D_1^2-2S_1^2+D_2^2-S_2^2\right)+V(1-4D_2^2)\right]+\frac{N}{4}\left(K+\delta K\sin^2\xi\right)u_{\rm t}^2, \tag{5}$$

where $\varepsilon_k=-2t\cos k$ and

$$\Delta_{Q_0,\sigma}=\frac{U}{2}D_{Q_0}-{\rm sgn}(\sigma)\frac{U}{2}S_{Q_0}, \tag{6}$$

$$\Delta_{2Q_0,\sigma}=\left(\frac{U}{2}-2V\right)D_{2Q_0}-{\rm sgn}(\sigma)\frac{U}{2}S_{2Q_0}. \tag{7}$$

The total energy is given by $E(u_{\rm t},\xi)=\langle H_{\rm MF}\rangle_{\rm MF}/N$, where $\langle\cdots\rangle_{\rm MF}$ is the expectation value over the mean-field Hamiltonian. The ground-state energy is obtained by minimizing the total energy with respect to $u_{\rm t}$ and ξ, where the corresponding equations are obtained as

$$(K+\delta K\sin^2\xi)u_{\rm t}$$
$$={\rm e}^{{\rm i}\xi}\frac{-1+{\rm i}}{N}\sum_{k,\sigma}(\cos k-\sin k)\left\langle c^\dagger_{k\sigma}c_{k+Q_0,\sigma}\right\rangle_{\rm MF}+{\rm c.c.}, \tag{8}$$

$$-\frac{\delta K}{2}u_{\rm t}\sin(2\xi)$$
$$={\rm e}^{{\rm i}\xi}\frac{1+{\rm i}}{N}\sum_{k,\sigma}(\cos k-\sin k)\left\langle c^\dagger_{k\sigma}c_{k+Q_0,\sigma}\right\rangle_{\rm MF}+{\rm c.c.}. \tag{9}$$

The parameters D_1, D_2, S_1, S_2, $u_{\rm t}$, θ, θ', and ξ are evaluated self consistently using eqs. (3), (4), (8), and (9). We also examine $E(u_{\rm t},\xi)$ to investigate the possible metastable state at $u_{\rm t}=0$. The present calculation has been performed for $U=3$, where we take the hopping energy t as unity.

In Fig. 1, we present the states obtained in our Hamiltonian. Two kinds of phases of ξ and θ correspond to those of order parameters for the lattice tetramerization and the $2k_{\rm F}$ SDW, respectively:

$$u_{\rm t}\cos\left(\frac{\pi}{2}j+\xi\right),\quad S_1{\rm e}^{{\rm i}\theta}.$$

The symbol $*$ in Fig. 1 implies the state with $u_{\rm t}=0$. The SDW + CO (D_2+S_1) is the charge-ordered state with the alternation of the charge-rich/poor sites. The pure SDW (S_1) has a spin amplitude, the maximum of which is located on the bonds in order to gain the transfer energy. Both the SDW+CO state and the SDW state do not have any lattice distortion, namely, $u_{\rm t}=0$. The bond-centered CDW and site-centered CDW states are the Peierls states, i.e., the nonmagnetic states with finite lattice distortion (tetramerization) and with $2k_{\rm F}$ charge modulations. The lattice tetramerization takes the maximum amplitude on the bonds in the former state, while it does so on the sites in the latter state. We note that all these states exhibit the insulating behavior due to the presence of the $2k_{\rm F}$ density wave (S_1 or D_1), which yields the gap in the dispersion at the Fermi energy.

We note the relevance of the present analysis to the state of the quasi-one-dimensional (EDO-TTF)$_2$PF$_6$ compound. The

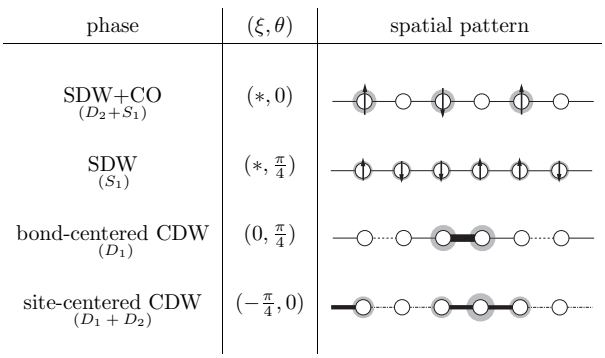

Fig. 1. Several possible ordered states obtained in the present model. The notation (ξ,θ) denotes the set of the phases for the lattice tetramerization ($u_j=u_{\rm t}\cos(\pi j/2+\xi)$) and for the order parameter of the SDW ($S_1{\rm e}^{{\rm i}\theta}$) or the CDW ($D_1{\rm e}^{{\rm i}(\pi/2+\theta)}$). The circle with the shaded region denotes charge-rich sites and the bold line corresponds to the bond with large transfer energy.

Peierls state observed at low temperatures is precisely of the bond-centered CDW type.[11] Therefore, in the present paper, such a type of the CDW is mainly examined to find the possible metastable state, which could be the origin of the photoinduced phase realized after releasing the lattice distortion.

3. Effect of Alternating Elastic Constant on Ground State

In order to clarify the starting point of the present work, we begin to examine the case for $\delta K = 0$, in which some results can be compared with the previous works.

First, we briefly recall the electronic state in the absence of the e-p interaction.[5] There is a critical value $V_c \simeq 0.28$ where the state with $S_1 \neq 0$ and $D_2 = 0$ is obtained for $V < V_c$, and that with $S_1 \neq 0$ and $D_2 \neq 0$ is obtained for $V > V_c$. The CO state for $V > V_c$ has a charge disproportionation with two-fold periodicity (Fig. 1). The phase transition at $V = V_c$ is of the first order where the both order parameters D_2 and S_1 exhibit discontinuous change. The difference in SDW (S_1) between the case of $V < V_c$ and that of $V > V_c$ is that the maximum of the spin amplitude is on the bonds in the former case while it is on the sites in the latter case. Such a difference can be understood from the commensurability energy for the $2k_F$ SDW ($S_{Q_0} \equiv S_1 e^{i\theta}$) at quarter filling, which decreases continuously and vanishes only at $V = V_c$. Actually, the θ dependence of eq. (5) takes the form[19]

$$E_g(\theta) = \text{const.} + C(V)\cos 4\theta, \tag{10}$$

where the V dependence of $C(V)$ is given by $C(V) = C_{00} - C_{01}V - C_{03}V^3 + \cdots$ with C_{0j} being positive numbers. Thus, one finds $C(V) > 0$, i.e., $\theta = \pi/4$ (bond-centered density wave), for $V < V_c$, while one finds $C(V) < 0$, i.e., $\theta = 0$ (site-centered density wave), for $V > V_c$. We note that, due to such a sign change of $C(V)$, the collective mode for the phase fluctuation exhibits the vanishing of the commensurability gap at $V = V_c$ leading to the metallic property. In fact, a noticeable behavior emerges in the optical conductivity $\sigma(\omega)$ (ω being the frequency), where the static conductivity $\sigma(0)$ becomes finite at $V = V_c$ even for the commensurate SDW state.[20]

Next, we consider the case with the e-p coupling but with $\delta K = 0$. In Fig. 2, we show the phase diagram of the ground states obtained from eqs. (3), (4), (8), and (9). The bold line denotes the boundary for the first-order phase transition, which is estimated by comparing the minimum energy of $E(u_t, \xi)$. For large K (i.e., for small e-p coupling), we obtain $u_t = 0$ and there is a critical value $V_c \simeq 0.28$, where the SDW state is obtained for $V < V_c$ and the SDW+CO state is obtained for $V > V_c$. With decreasing K, the state with finite lattice tetramerization ($u_t \neq 0$) appears. There is the $D_1 + S_1$ state in between the SDW state and the bond-centered CDW state, where both boundaries do not depend on V. Such a V-independent result is ascribed to the mean-field treatment in which V does not contribute to the mean field for S_1 and D_1 [see eqs. (6) and (7)]. For the intermediate K and small V, there exists the region of the bond-centered CDW. This state resembles the BCDW state suggested by Clay *et al*. (Fig. 3(b) and Fig. 4 in ref. 18) and the DM+SP state suggested by Kuwabara *et al*. (Fig. 2 in ref. 15), in the sense that the amplitude of the lattice tetramerization takes a maximum on the bonds; i.e., bond-centered state.

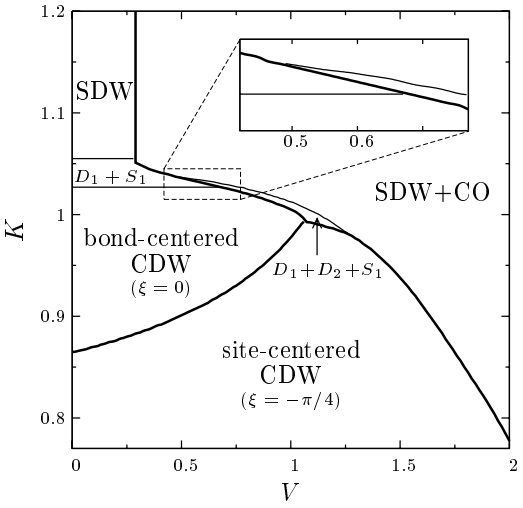

Fig. 2. Phase diagram on the plane of V and K for $\delta K = 0$ and $U = 3$. The bold (thin) solid line corresponds to the first- (second-)order phase transition. The region framed by the dotted rectangle is enlarged to show clearly several kinds of phases.

Here, we note the effects of the quantum fluctuation and the lattice dimerization, which are not taken into account in the present mean-field treatment. It is possible that the magnetic state of the SDW+CO turns into a nonmagnetic state in the presence of the quantum fluctuation and the e-p coupling. Compared with the case in ref. 15, the mean field stabilizes the CO and the charge disproportionation in which the strong correlation and the quantum fluctuations take important roles. Thus, in the mean-field treatment, the boundary between the bond-centered CDW state and the site-centered CDW state is shifted to the weak coupling region, and the SDW+CO state is stabilized for relatively small V. It is also expected that, due the quantum effect, the boundary between the SDW+CO and site-centered CDW states becomes a crossover and the nonmagnetic state would be realized in both regions. Furthermore the lattice dimerization can be expected to coexist with the bond-centered CDW state.[15,18] In the sense of the variational principle, the region for the bond-centered CDW is extended by introducing the lattice dimerization.

The bond-centered CDW state originates from the facts that the on-site repulsive interaction U separates two electrons being on the same site, and that the bond-centered ordering gives rise to the large gain of the transfer energy. For large V, the site-centered CDW state is realized in order to avoid the increase in the energy of V. As seen from Fig. 1, the site-centered CDW state takes a maximum of the charge on the sites, where the gain of the transfer energy is made favorable owing to the electron hopping into both nearest sites. This state would correspond to the $4k_F$ CDW-SP state suggested by Clay *et al.* (Fig. 3(d) in ref. 18) and the CO+SP state suggested by Kuwabara *et al.*,[15] since the lattice tetramerization takes the maximum amplitude on the sites. We note that, in the present case, the maximum of charge is located on the same position as that of lattice tetramerization (i.e., the amplitude of D_1 is larger than that of D_2). However, for the state in ref. 15, the maximum is obtained at the same position as that of the $4k_F$ CDW (i.e., the amplitude of D_2 is larger than D_1). This may originate from our choice of relatively small U

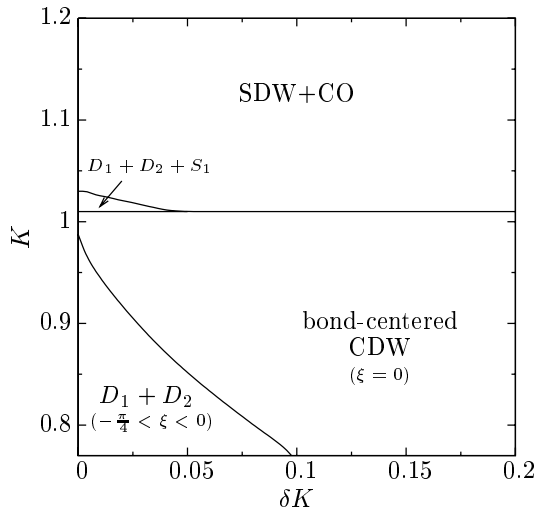

Fig. 3. Phase diagram on the plane of δK and K for $U=3$ and $V=1$. The narrow region for small δK and around $K\simeq 1.03$ is characterized by $D_1+D_2+S_1$ (see Fig. 2). With increasing δK, the region D_1 (bond-centered CDW) extends while that for D_1+D_2 (site-centered CDW) diminishes. For $\delta K\neq 0$, the D_1+D_2 state takes ξ with an intermediate value of $-\pi/4<\xi<0$.

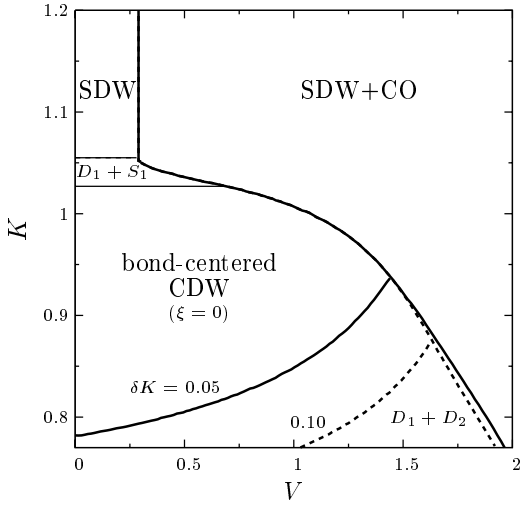

Fig. 4. Phase diagram on the plane of V and K with several choices of $\delta K=0.05$ and 0.1. The phase boundaries for finite δK are shown by the dotted line ($\delta K=0.05$) and the dashed line ($\delta K=0.10$). The region of the bond-centered CDW (D_1) state is enlarged with increasing δK. For $\delta K\neq 0$, the state D_1+D_2 takes ξ with an intermediate value of $-\pi/4<\xi<0$.

and then our site-centered CDW state is expected to move to the CO+SP state for large U.

Now we show how the site-centered CDW (D_1+D_2) diminishes when δK increases from zero. In Fig. 3, the variations of the D_1+D_2 state and the bond-centered CDW (D_1) are shown as a function of δK. The SDW+CO (D_2+S_1) remains unchanged since $u_t=0$. The addition of the δK term increases the energy of the D_1+D_2 state with $\xi\neq 0$, but does not affect on the D_1 state with $\xi=0$. Thus, the change from the D_1+D_2 state into the D_1 state occurs with increasing δK. In the phase diagram of Fig. 4, the boundaries between the D_1+D_2 state and the D_1 state are shown for the choices of $\delta K=0.05$ and 0.1. The region of bond-centered CDW increases rapidly with increasing δK, i.e., a small amount of δK is enough to obtain the bond-centered CDW state as the ground state. It is noticed that the boundary of the direct transition from the bond-centered CDW state to the SDW+CO state emerges even for $\delta K=0.05$. Such a boundary is in contrast to that in Fig. 2.

Here, we compare the experimental findings in the (EDO-TTF)$_2$PF$_6$ compound with the results of the present calculation. The Peierls state observed in (EDO-TTF)$_2$PF$_6$ is of the type of the bond-centered CDW,[13] and the photoinduced phase transition from the Peierls insulator to a metal takes place by the weak laser photoexcitation. This behavior has been discussed by assuming the metastable state without lattice distortion.[11] In our calculation, the bond-centered CDW state is actually reproduced in Figs. 2 and 4. One can expect the metastable state in the region near the boundary between the the bond-centered CDW state and the undistorted state, since the the phase transitions are of the first order. Thus, we focus on the properties of the first-order phase transitions from the bond-centered CDW state to the SDW+CO state. From the inset of Fig. 2, it can be seen that the system does not show a direct transition between the bond-centered CDW state and the SDW+CO state, but there are intermediate states between these two states. Actually, the following three types of transitions occur when the bond-centered CDW state moves to the SDW+CO state with increasing K. (i) For $0.67\lesssim V\lesssim 1.06$, the bond-centered CDW state shows a first-order phase transition to the $D_1+D_2+S_1$ state and undergoes a second-order transition to the SDW+CO state. (ii) For $0.49\lesssim V\lesssim 0.67$, the bond-centered CDW state shows a second-order transition to the D_1+S_1 state followed by the successive transitions of a first-order one into the $D_1+D_2+S_1$ state and a second-order one into the SDW+CO state. (iii) For $0.28\lesssim V\lesssim 0.49$, the bond-centered CDW state shows a second-order transition to the D_1+S_1 state and then undergoes a first-order transition to the SDW+CO state. The first-order phase transition in case (i) can be ascribed to the difference between the symmetry in the bond-centered CDW ($\xi=0$) and that in the $D_1+D_2+S_1$ state ($\xi=-\pi/4$), where both states have finite lattice distortion. The origin of the first-order transition in case (ii) is also the same as that in case (i). In these cases, the second-order transition between the $D_1+D_2+S_2$ state with $\xi=-\pi/4$ and the SDW + CO state implies that the state around $u_t=0$ is unstable and turns out to be irrelevant to (EDO-TTF)$_2$PF$_6$. For case (iii), the first-order transition is due to the difference in the locking of the phase θ, i.e., $\theta=\pi/4$ in the D_1+S_1 state and $\theta=0$ in the SDW+CO state. This case is also irrelevant to the state of the (EDO-TTF)$_2$PF$_6$, since the spin ordering is absent in the Peierls state. Thus, both the metastable state at $u_t=0$ and the ground state of the bond-centered CDW ($u_t\neq 0$) cannot be explained within the model of $\delta K=0$, suggesting a new mechanism for the photoinduced phase observed in the (EDO-TTF)$_2$PF$_6$ compound. Our idea is the introduction of the alternation of the elastic constant, which enables us to reproduce the experimental findings. By increasing δK, the region of the bond-centered CDW state is enhanced and moreover, there is a direct first-order phase transition to the lattice-undistorted SDW+CO state, as seen from Fig. 4. Such a behavior comes from the fact that the δK has a role of fixing the phase $\xi=0$,

which can be obtained from eq. (5). On the basis of such a consideration, we examine the bond-centered CDW state and the mechanism of the emergence of the metastable state at $u_t = 0$ by setting $\xi = 0$ in the next section. We discuss the relevance to the (EDO-TTF)$_2$PF$_6$ compound in §5.

4. Phase Diagram and Metastable State for Large δK

In the following calculation, we examine the case of $\xi = 0$ corresponding to the bond-centered lattice distortion, which is realized by choosing a moderate magnitude of $\delta K \geq 0.2$ as shown in the preceding section. The neglect of the lattice dimerization can be justified by considering the large δK, as will be discussed in §5.

In order to understand the role of the e-p interaction in the correlated system, we first examine eq. (5) by treating u_t as an external field, i.e., by discarding the condition of eqs. (8) and (9). We calculate the order parameters S_j and D_j ($j = 1, 2$) as a function of u_t. The CDW, whose order parameter D_1 is always finite due to the presence of the external field u_t, is called the extrinsic $2k_F$ charge-density wave (ECDW). In Fig. 5, we explain how the state varies with increasing u_t. When $V = 0$, the order parameter S_1 decreases monotonically and becomes zero at $u_t \approx 0.5$. For $V = 1$, both the order parameters D_2 and S_1 take finite values for $u_t = 0$, but as u_t increases, D_2 decreases rapidly and becomes zero at $u_t \approx 0.26$ and S_1 becomes zero at $u_t \approx 0.5$. The $D_1 + S_1$ state is understood by noting that S_1 is rather robust compared with D_2 because $U > V$. With increasing u_t ($0.28 < V$), the phase of the SDW, θ, increases from zero and reaches $\pi/4$ at which D_2 vanishes. Such a variation of θ comes from the competition of D_2 and D_1. We obtain $\theta' = \theta + \pi/2$ for the $D_1 + S_1$ state and the D_1 state. For larger values of $V(\gtrsim 1.5)$, the strong competition of D_2 and u_t results in the first-order transition, which is followed by the discontinuous changes of S_j and D_j ($j = 1, 2$). Furthermore, for $V(\gtrsim 1.7)$, the vanishing of D_2 and S_1 takes place simultaneously due to the strong effect of u_t.

The phase diagram is summarized in Fig. 5. The second-order and first-order transitions take place at the boundaries of the thin and bold lines, respectively, where the point with $u_t = 0$ and $V = V_c(\simeq 0.28)$ is the singular one showing the first-order transition of D_2. For the coexistent state of $D_1 + D_2 + S_1 + S_2$, both the amplitudes S_1 and D_2 are larger than that of D_1. In the $D_1 + S_1$ state, the amplitude of S_1 is larger than that of D_1. For large u_t, the pure ECDW (D_1) state appears, e.g., for $u_t \gtrsim 0.5$ and $V \lesssim 1.7$. The boundary between the $D_1 + S_1$ state and the $D_1 + D_2 + S_1 + S_2$ state in the region of $0.5 \lesssim V \lesssim 1.5$ is given by $V \simeq 4u_t$, indicating a direct competition between u_t and V. On the boundary corresponding to the vanishing of D_2, one sees a point where the second-order transition changes into the first-order transition with increasing V. This variation resembles that found in the phase diagram in the V versus temperature (instead of u_t) plane.[10] Such a fact may be explained by the existence of the term proportional to $D_2 S_1^2$ in the energy expansion with respect to the order parameter.[10] The solid line of the phase boundary between the D_1 state and the $D_1 + D_2 + S_1 + S_2$ state is given by $u_t \simeq \frac{2}{3}V - 0.8$ for $V \gtrsim 1.7$. We found that D_1 is always finite due to the external field u_t, but is strongly suppressed in the presence of D_2 (not shown), i.e., the strong competition between D_2 and D_1, which is a characteristic of 1/4-filled systems. Also note that $\theta = \pi/4$ if $D_2 = 0$; i.e., the maximum density is located on the bonds in the absence of CO.

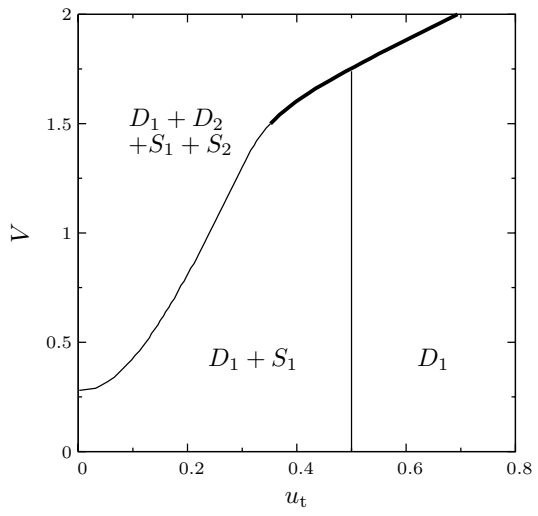

Fig. 5. Phase diagram on the plane of u_t and V where u_t is regarded as an external field (see text). The thin and bold lines correspond to the boundaries of the second-order and first-order transitions, respectively. Order parameters S_1, D_1, D_2 represent SDW, ECDW and CO, respectively.

Next we examine the u_t dependence of the mean-field energy $E(u_t)$, which is defined by $E(u_t, \xi = 0)$. The minimum of this energy gives the true ground-state energy. In Fig. 6, the energy difference, $\delta E(u_t) \equiv E(u_t) - E(0)$, is shown as a function of u_t for $V = 0.1$ with some choices of K. This behavior denotes the conventional second-order phase transition except for its having several kinds of order parameters, S_1 and D_1. For $K = 1.06$, the minimum is obtained at $u_t = 0$ corresponding to the pure SDW state. The closed circle at $u_t \simeq 0.5$ denotes the point where the S_1 state vanishes. Thus, we obtain the SDW (S_1) state for $K \gtrsim 1.05$, the $D_1 + S_1$ state for $1.03 \lesssim K \lesssim 1.05$, and the pure bond-centered CDW (D_1) state for $K \lesssim 1.03$. Figure 7 shows the case for $V = 1$. The novel feature in $\delta E(u_t)$ compared with that of Fig. 6 is the emergence of a local minimum at $u_t = 0$. For $0.79 \lesssim K \lesssim 1.01$, we find a metastable state where the energy of the local minimum $E(u_t = 0)$ is larger than the energy of the true minimum at finite u_t. This fact implies that, with decreasing K, the system exhibits the first-order phase transition from the SDW+CO ($D_2 + S_1$) state into the bond-centered CDW state at $K \approx 1.01$. We note that, for $0.28 \lesssim V \lesssim 0.70$, there is a very narrow region of K around $K \approx 1.03$ for the $D_1 + S_1$ state (not shown), as found in Fig. 4. For a larger choice of $V = 1.6$, the local minimum at $u_t = 0$ is found for $0.6 \lesssim K \lesssim 0.89$.

Here, we examine the origin of the metastable state found in Fig. 7. The mean-field energy of eq. (5) can be expanded in terms of u_t as

$$E(u_t) = E(0) + \left(\alpha + \frac{1}{4}K\right) u_t^2 + \beta u_t^4 + \cdots . \tag{11}$$

The coefficients, α and β, can be estimated numerically and are shown in Fig. 8 as a function of V. With increasing V, there is a jump in both α and β at $V = V_c(\simeq 0.28)$, at which the pure SDW state moves to the SDW+CO state; i.e., the D_2 state emerges. It can be found that $\alpha < 0$ for arbitrary V, and that $\beta < 0$ ($\beta > 0$) for $V > V_c$ ($V < V_c$). The result of $\alpha < 0$ is quite reasonable when we note that u_t acts as the external

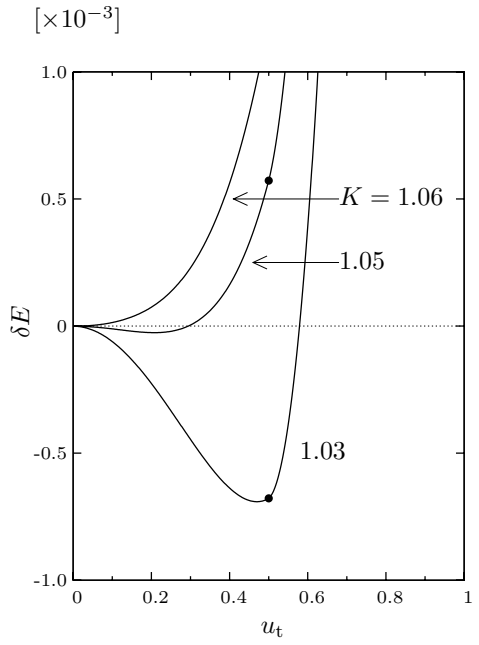

Fig. 6. u_t dependence of $\delta E(u_t)(\equiv E(u_t)-E(0))$ for $V=0.1$ with fixed $K=1.03$, 1.05, and 1.06. With increasing u_t, S_1 decreases and vanishes at the point shown by the closed circle.

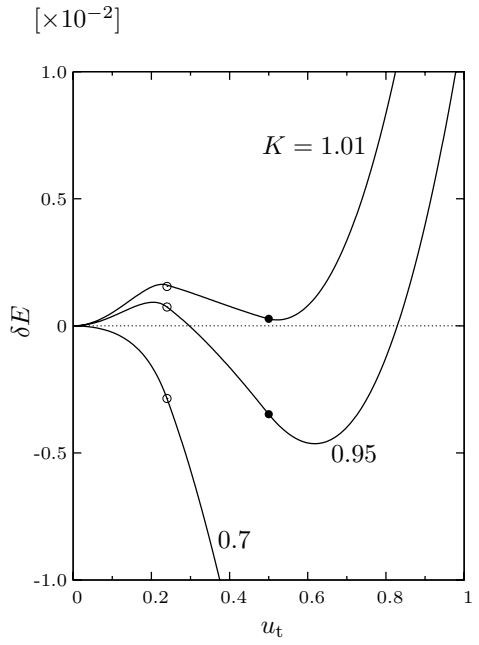

Fig. 7. u_t dependence of $\delta E(u_t)$ for $V=1$ with fixed $K=0.70$, 0.95, and 1.01. With increasing u_t, D_2 (S_1) decreases and vanishes at the point shown by the open (closed) circle.

field. In order to understand why β is negative and diverges as $V \to V_c+0$, we examine eq. (5) in terms of the phase degrees of freedom θ.[10] Actually, from eq. (5), the energy with fixed u_t and θ is expressed as

$$E(u_t,\theta) = E_g(\theta) + \left(\alpha' - \gamma\sin 2\theta + \frac{1}{4}K\right)u_t^2 + \beta' u_t^4 + \cdots, \tag{12}$$

where $E_g(\theta)$ is given by eq. (10). Quantities $\alpha'(<0)$, $\beta'(>0)$,

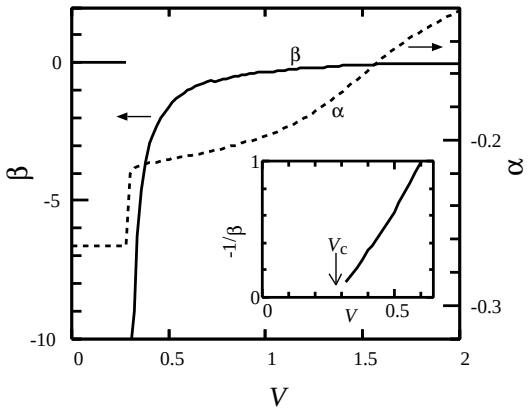

Fig. 8. V dependence of α and β in eq. (11), where $\theta=\pi/4$ (0) for $V<V_c$ ($V>V_c$). The inset denotes $-1/\beta$, which is proportional to $(V-V_c)$ for $V>V_c$.

and $\gamma(>0)$ are estimated numerically from eq. (5). The γ-term, which is proportional to S_1^2, denotes the interaction between the bond-centered CDW (D_1) state and the SDW (S_1) state. The coefficients are estimated as $\alpha' \simeq -0.197$, $\beta'=0.0068$, and $\gamma \simeq 0.056$ for $V=1$, where $\beta' \simeq 0.0145$ for $V<V_c$. There is a small jump of γ at $V=V_c$, where the V dependence of γ is much smaller than that of α. The locking position of θ can be determined in order to minimize eq. (12). The commensurability potential $E_g(\theta)$ for $V>V_c$ favors the locking position $\theta=0$, while the γ-term favors $\theta=\pi/4$. For $V>V_c$, by minimizing eq. (12) with respect to θ, we obtain eq. (11) with the coefficients

$$\alpha=\alpha', \qquad \beta=\beta'-\frac{\gamma^2}{8|C(V)|}. \tag{13}$$

We can immediately reproduce the anomalous behavior $-1/\beta \propto (V-V_c)$ at $V=V_c+0$, by noting that the coefficient $C(V)$ follows $C(V)\propto(V-V_c)$. This is the reason why the coefficient of the fourth-order term β can become negative for $V>V_c$. It is shown that the result similar to eq. (13) can be obtained from the bosonization scheme, in which the spin degree of freedom is also taken into account.[21] For $V<V_c$, the γ-term does not contribute to the u_t^4 term since both the commensurability potential and the γ term favors the locking position $\theta=\pi/4$ (one simply obtains $\alpha=\alpha'-\gamma$). Thus, the conventional second-order transition is reproduced. From these arguments, the conditions for the metastable state are summarized as follows: *(i) the existence of the CO for $V>V_c$ (the commensurability energy leading to $\theta=0$), (ii) the coupling between the SDW state (S_1) and the bond-centered CDW state (u_t), which is given by the γ term in eq. (12), and (iii) the mechanism to fix $\xi=0$ as discussed in §3.*

Finally we show the phase diagram of the ground state on the plane of V and K in Fig. 9. For $K \gtrsim 1.05$ corresponding to the weak e-p coupling, we obtain either the pure SDW ($V<V_c$) with $\theta=\pi/4$ or the SDW+CO ($V>V_c$) with $\theta=0$. With decreasing K (i.e., increasing the e-p coupling), the bond-centered CDW state with $\theta=\pi/4$ appears for $K<K_c$ where K_c is a critical value of the first-order phase transition for the Peierls state. The state with $u_t=0$ becomes metastable in the large interval region of $K<K_c$ as shown by the shaded

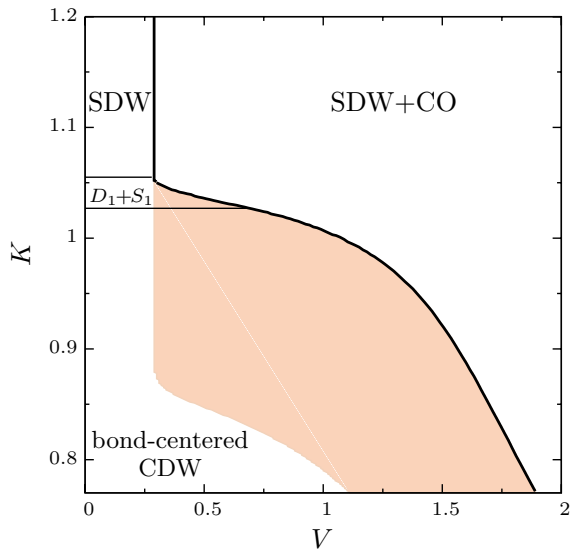

Fig. 9. (Color online) Phase diagram of the bond-centered CDW (D_1), SDW+CO (D_2+S_1), SDW (S_1), and bond-centered-CDW+SDW (D_1+S_1) states, on the plane of V and K. The shaded region denotes the area where the metastable state at $u_t = 0$ appears. The thin and bold lines correspond to phase boundaries of the second-order and first-order transitions, respectively.

area. The lower boundary of the shaded region is given by

$$K = -4\alpha, \tag{14}$$

which is verified from α in Fig. 8. There is also another metastable state with the local minimum at $u_t \neq 0$, which is located in a certain region of $K > K_c$ (not shown in Fig. 9).

5. Summary and Discussion

We examined the Peierls-Hubbard model at quarter-filling with the intersite interaction (V), and obtained the ground-state phase diagram within the mean-field theory. A noticeable finding is the undistorted state ($u_t = 0$), which becomes metastable in the bond-centered CDW state close to the boundary between the bond-centered CDW state and the SDW+CO state. The obtained bond-centered CDW ground state and its metastable state may share the following common features with the Peierls state of the (EDO-TTF)$_2$PF$_6$ compound. The spatial variation of the Peierls state is the same, and the metastable state for $u_t = 0$ could be related to the photoinduced phase found in the experiment on the EDO-TTF compound.

In the present analysis of §4, we assumed $\xi = 0$ in order to stabilize the bond-centered CDW state and examined the metastable state at $u_t = 0$, which may be relevant to the property of the EDO-TTF compound. Actually, in the normal state of this compound, there is the alternation of the bending of the molecule for every two sites along the the one-dimensional chain.[12] In addition to the ground state (§3), we discuss this assumption for the metastable state on the basis of the energy, which is expanded in terms of u_t. The energy with fixed u_t, θ, and ξ can be explicitly written as

$$E(u_t,\theta,\xi) = C(V)\cos 4\theta + \left(\alpha' - \gamma\sin(2\theta - 2\xi)\right)u_t^2 + \left(\frac{K}{2} + \frac{\delta K}{4}\sin^2\xi\right)u_t^2 + \cdots, \tag{15}$$

where the δK term denotes an increase in elastic energy for $\xi \neq 0$. Here, we note that, even for $V > V_c$, there is no competition between θ and ξ for $\delta K = 0$, since the minimum of eq. (15) is obtained by choosing ξ so as to satisfy $\sin(2\theta - 2\xi) = 1$. In this case, the $\gamma^2/C(V)$ term in β [see eq. (13)] is absent and the energy $E(u_t,\theta,\xi)$ [eq. (15)] takes a true minimum at $u_t = 0$ (i.e., $\beta > 0$). When $\delta K \neq 0$, the energy $E(u_t,\theta,\xi)$ as a function of ξ increases and the metastable state around $u_t = 0$ can be expected (i.e., $\beta < 0$). Actually, for $\delta K > 0.46$, the energy $E(u_t,\theta,\xi)$ takes a local minimum at $u_t = 0$ for all values of ξ, in the case of $K = 0.9$ and $V = 1$. Thus, the assumption $\xi = 0$ can be justified when the degree of alternation of the elastic constant δK becomes larger than a critical value.

In the present analysis, we did not consider the possibility of lattice dimerization ($u_j = (-1)^j u_d$, where u_d is the amplitude of the lattice dimerization). Since the elastic energy of the lattice dimerization is given by $(N/2)(K + \delta K/2)u_d^2$, δK also has an effect of suppressing the lattice dimerization. From these arguments, we expect that the effect of δK will arise from the bending freedom of the molecules in the (EDO-TTF)$_2$PF$_6$ compound. Such a bending plays important roles in the photoinduced cooperative transition, although the origin of the molecular property still remains an open question from a microscopic view point.

Here, we note states at finite temperatures. There are some theoretical works on finite-temperature properties. Quite recently, it has been pointed out that the Peierls-Hubbard model with $\delta K = 0$ exhibits the first-order transition from the dimer-Mott state into the spin-Peierls state,[22] where both states show the insulating behavior. On the other hand, the purely electronic model shows the transition from the metallic state into the insulating state of the $2k_F$ SDW + $4k_F$ SDW + $2k_F$ CDW state.[10] Compared with the state of the (EDO-TTF)$_2$PF$_6$ compound, the normal state at high temperatures is different from the dimer-Mott state obtained from the former model and the lattice deformation cannot be reproduced in the latter model. It is expected that the parameters in the shaded region in Fig. 9 will lead the first-order phase transition into the normal state with increasing temperature, and that such a transition will be strongly enhanced by the effect of the large bending of molecules in the (EDO-TTF)$_2$PF$_6$.

Acknowledgements

The authors thank Professors H. Yamochi, G. Saito, S. Koshihara, K. Yonemitsu, J.-F. Halet, and L. Ouahab, and Drs. Y. Nakano, K. Onda, A. Ota, and H. Seo, for useful discussions and comments. The present work has been financially supported by a Grant-in-Aid for Scientific Research on Priority Areas of Molecular Conductors (No. 15073213) from the Ministry of Education, Culture, Sports, Science and Technology, Japan, and by the JSPS Core-to-Core Program Project "Multifunctional Molecular Materials and Device Applications".

1) D. Jérome and H. J. Schulz: Adv. Phys. **31** (1982) 299.
2) G. Grüner: Rev. Mod. Phys. **66** (1994) 1.
3) V. J. Emery: *Highly Conducting One-Dimensional Solids*, eds. J. T. Devreese, R. P. Evrard, and V. E. van Doren (Plenum, New York, 1979).
4) H. Yoshioka, M. Tsuchiizu, and Y. Suzumura: J. Phys. Soc. Jpn. **69** (2000) 651.

5) H. Seo and H. Fukuyama: J. Phys. Soc. Jpn. **66** (1997) 1249.
6) J. P. Pouget and S. Ravy: J. Phys. I France **6** (1996) 1501, Synth. Metals **85** (1997) 1523.
7) S. Kagoshima, Y. Saso, M. Maesato, R. Kondo, and T. Hasegawa: Solid State Commun. **110** (1999) 479.
8) N. Kobayashi, M. Ogata, and K. Yonemitsu: J. Phys. Soc. Jpn. **67** (1998) 1098.
9) Y. Tomio and Y. Suzumura: J. Phys. Soc. Jpn. **69** (2000) 796.
10) Y. Tomio and Y. Suzumura: J. Phys. Chem. Solids **62** (2001) 431.
11) M. Chollet, L. Guerin, N. Uchida, S. Fukaya, H. Shimoda, T. Ishikawa, K. Matsuda, T. Hasegawa, A. Ota, H. Yamochi, G. Saito, R. Tazaki, S. Adachi, and S. Koshihara: Science **307** (2005) 86.
12) A. Ota, H. Yamochi, and G. Saito: J. Mater. Chem. **12** (2002) 2600.
13) O. Drozdova, K. Yakushi, K. Yamamoto, A. Ota, H. Yamochi, G. Saito, H. Tashiro, and D.B. Tanner: Phys. Rev. B **70** (2004) 075107.
14) K. Onda, T. Ishikawa, M. Chollet X. Shao, H. Yamochi, G. Saito, and S. Koshihara: J. Phys. Conf. Series **21** (2005) 216.
15) M. Kuwabara, H. Seo, and M. Ogata: J. Phys. Soc. Jpn. **72** (2003) 225.
16) W. P. Su, J. R. Schrieffer, and A. J. Heeger: Phys. Rev. Lett. **42** (1979) 1698.
17) H. Fukuyama and H. Takayama: in *Dynamical Properties of Quasi-One-Dimensional Conductors - Phase Hamiltonian Approach in Electronic Properties of Inorganic Quasi-One-Dimensional Compounds* -, ed. P. Monceau (D. Reidel Publishing 1985), p. 41.
18) R.T. Clay, S. Mazumdar, and D. K. Campbell: Phys. Rev. B **67** (2003) 115121.
19) Y. Suzumura: J. Phys. Soc. Jpn. **66** (1997) 3244.
20) Y. Tomio and Y. Suzumura: J. Phys. Soc. Jpn. **71** (2002) 2742.
21) M. Tsuchiizu and Y. Suzumura: arXiv:0801.1891.
22) H. Seo, Y. Motome, and T. Kato: J. Phys. Soc. Jpn. **76** (2007) 013707.